Electronic Supplementary Material (ESI) for Chemical Communications

Monitoring the On/Off Switching of the Electronic Communication in Diethynylplatinum(II)-bridged Dyads Using Triplet Energy Transfer

Ahmed M. Soliman, Mohammed Abdelhameed, Eli Zysman-Colman and Pierre D. Harvey**

Département de chimie, Université de Sherbrooke,
2500 Boul. Université, Sherbrooke, QC, J1K 2R1

Pierre.Harvey@usherbrooke.ca; Eli.Zysman-Colman@usherbrooke.ca

SUPPORTING INFORMATION

Table of Contents: **Pages**

Experimental section

Synthesis: General Procedures:

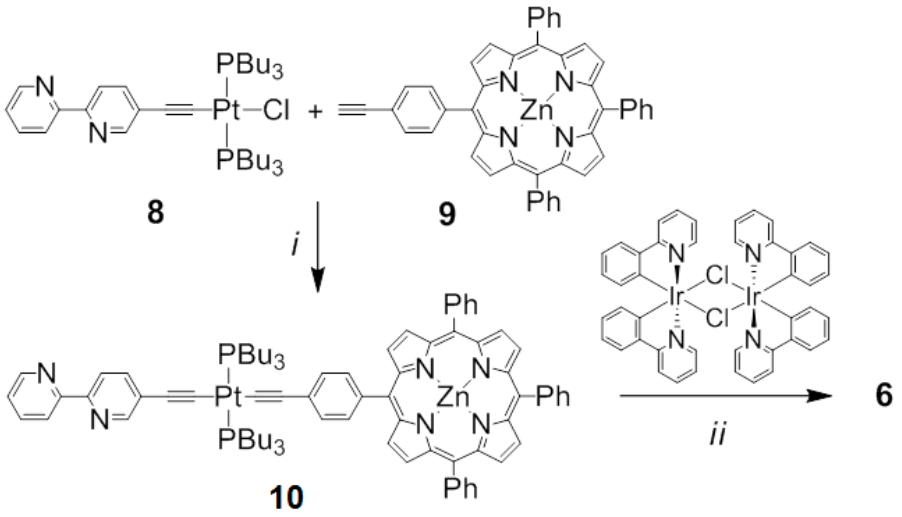

Commercial chemicals were used as supplied. All experiments were carried out with freshly distilled anhydrous solvents obtained from a Pure Solv™ solvent purification system from Innovative Technologies except where specifically mentioned. *N*,*N*,*N*-Triethylamine (Et_3N), *N*,*N*-di*iso*propylamine (*i*-Pr_2NH) were distilled over CaH_2 under a nitrogen atmosphere. $PtCl_2(PBu_3)_2$ was obtained following standard literature protocol[1] and heated to 165 °C to obtain the *trans* form. CuI,[2] $[(ppy)_2Ir\text{-}\mu\text{-}Cl]_2$ dimer,[3] *trans*-(5-ethynyl-2,2'-bipyridine)-chloro-bis(tri-*n*-butylphosphine)platinum (**8**)[4] and 5-(4-ethynylphenyl)-10,15,20-trisphenylporphyrin-zinc(II)(**9**)[5] were prepared following literature procedures. All reagents wherein the synthesis is not explicitly described in the SI were purchased and used without further purification. Flash column chromatography was performed using silica gel (Silia-P from Silicycle, 60 Å, 40-63 μm). Analytical thin layer chromatography (TLC) was performed with silica plates with aluminum backings (250 μm with indicator F-254). Compounds were visualized under UV light. ^1H and ^{13}C NMR spectra were recorded on a Brucker Avance spectrometer at 400 MHz and 100 MHz, respectively or a Brucker Avance spectrometer at 300 MHz and 75MHz, respectively. ^{31}P NMR spectra were recorded on a Brucker Avance spectrometer at 121 MHz and 162 MHz, respectively. The following abbreviations have been used for multiplicity assignments: "s" for singlet, "d" for doublet, "t" for triplet and "m" for multiplet. Deuterated cholorform ($CDCl_3$) and deuterated acetonitrile (CD_3CN) were used as the solvent of record. Melting points (Mp's) were recorded using open end capillaries on a Meltemp melting point

apparatus and are uncorrected. High resolution mass spectra were recorded on a Waters Synapt MS G1 (ES-Q-TOF) at the Université de Sherbrooke.

Compound 10:

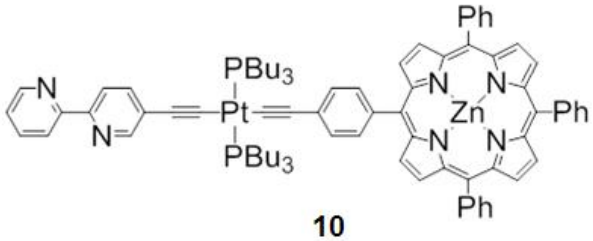

10

A dry flask charged with **8** (38 mg, 0.050 mmol, 1.1 equiv.) and CuI (2.0 mg, 0.010 mmol, 0.25 equiv.) in DCM (15 mL) and *i*-Pr_2NH (7.0 mL) was purged with N_2 for 30 min. Compound **9** (30 mg, 0.04 mmol, 1.0 equiv.), dissolved in DCM (7.0 mL), was then added. The mixture was stirred at room temperature for 20 h. The solvent was removed under reduced pressure and the residue was redissolved in DCM (30 ml). The organic phase was washed with H_2O twice then dried over $MgSO_4$ and concentrated under reduced pressure. The residue was purified by flash chromatography (10% EtOAc/Hexanes on silica gel) to yield 33 mg of violet solid (**Yield**: 48%). **^{1}H NMR (400 MHz, CD_3CN)** δ **(ppm):** 9.02 (d, *J* = 4.5 Hz, 2H), 8.95 (d, *J* = 5.4 Hz, 4H), 8.66 (d, *J* = 4.4 Hz, 1H), 8.63 (s, 1H), 8.36 (d, *J* = 7.9 Hz, 1H), 8.26 (d, *J* = 8.3 Hz, 2H), 8.22 (d, *J* = 6.6 Hz, 5H), 8.07 (d, *J* = 7.9 Hz, 2H), 7.84 – 7.72 (m, 8H), 7.72 – 7.63 (m, 4H), 7.31 – 7.23 (m, 4H), 2.35 – 2.21 (m, 12H), 1.79 – 1.65 (m, 12H), 1.62 – 1.52 (m, 12H), 1.01 (t, *J* = 7.3 Hz, 18H). **^{13}C NMR (75 MHz, CD_3CN)** δ**(ppm):** 156.3, 151.5, 151.2, 150.2, 150.1, 149.1, 142.8, 139.4, 138.2, 136.8, 134.4, 134.3, 132.0, 131.9, 127.4, 126.5, 125.9, 123.1, 121.0, 121.0, 120.8, 120.2, 110.1, 109.7, 109.3, 26.45, 24.50, 24.02, 13.90. **^{31}P NMR(162 MHz, CD_3CN)δ(ppm):** δ 3.58 (d, *J* = 2345.3 Hz). **LR-MS (**ES-Q-TOF**) (*m/z*):** 1479.6 (MH^+), 751.3. **HR-MS (**ES-Q-TOF**): Calculated** ($C_{82}H_{88}N_6P_2PtZn$)**:** 1479.5587 (MH^+), **Found**: 1479.5545 (MH^+).

Compound 6:

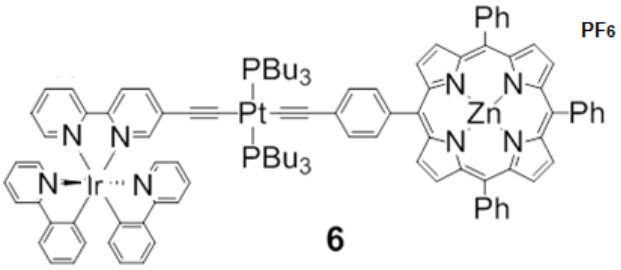

6

Iridium dimer $[(ppy)_2Ir(\mu\text{-}Cl)]_2$ (7 mg, 0.01 mmol, 0.5 equiv.) was dissolved in DCM (4.0 mL) and methanol (4.0 mL) and compound **10** (18 mg, 0.010 mmol, 1.0 equiv.) was added as a solid. The mixture was heated to 60 °C for 18 h at room temperature. The solution was cooled to RT and extracted with water (3 x 50 mL), then washed with ether (3 x 50 mL) to remove unreacted **10**. To the aqueous solution was slowly added a solution of NH_4PF_6 (10 mL, 10 % w/w in H_2O) under gentle stirring. The first drop caused the precipitation of an orange solid. The suspension was conserved at 0 °C for 2 h and then filtered and the resulting solid was washed with cold water to yield 12 mg of a violet solid (**Yield**: 93%). **^{1}H NMR (400 MHz, CD_3CN) δ (ppm):** 9.00 (d, *J* = 3.5 Hz, 2H), 8.94 (s, 4H), 8.64 (d, *J* = 8.0 Hz, 1H), 8.50 (d, *J* = 8.3 Hz, 1H), 8.22 (d, *J* = 6.6 Hz, 4H), 8.15 (t, *J* = 7.8 Hz, 2H), 8.07 (d, *J* = 7.3 Hz, 2H), 7.95 – 7.86 (m, 4H), 7.84 – 7.72 (m, 8H), 7.69 (d, *J* = 7.2 Hz, 2H), 7.62 (d, *J* = 7.4 Hz, 2H), 7.56 (dd, *J* = 8.6, 6.5 Hz, 2H), 7.35 (t, 2H), 7.26 (s, 4H), 7.12 – 6.97 (m, 4H), 6.98 (s, 1H), 6.92 (dd, *J* = 13.4, 6.7 Hz, 2H), 6.39 – 6.22 (m, 2H), 2.24 – 1.95 (m, 9H), 1.68 – 1.36 (m, 24H), 1.01 – 0.79 (m, 22H). **^{13}C NMR (75 MHz, CD_3CN) δ (ppm):** 167.9, 167.7, 156.0, 152.0, 150.8, 150.1, 149.9, 148.8, 148.5, 143.6, 143.4, 142.8, 140.2, 139.9, 139.7, 138.0, 137.9, 134.4, 134.3, 132.0, 131.7, 130.9, 130.6, 129.0, 127.5, 127.5, 126.5, 125.0, 124.7, 124.7, 124.6, 123.4, 123.1, 122.6, 122.3, 121.2, 121.1, 119.6, 119.4, 110.3, 110.0, 29.32, 26.37, 24.46, 23.91, 13.63. **^{31}P NMR(162 MHz, CD_3CN)δ(ppm):** 4.46 (d, *J* = 2315.8 Hz). **LR-MS** (ES-Q-TOF) **(*m/z*):** 1979.6(M^+), 1314.4, 1001.3. **HR-MS**(ES-Q-TOF) **Calculated**($C_{104}H_{104}IrN_8P_2PtZn$)**:** 1979.6426; **Found**: 1979.6416. Warning: During the course of this investigation, degradation of this compound was noticed yielding to modifications of the absorption and mass spectra. The latter exhibited a growing band at 620 nm upon prolonged time (months). This product could not be separated by column chromatography. All analyses were performed with freshly synthesized samples.

Photophysical characterization: All samples were prepared in 2-methyltetrahydrofuran (2-MeTHF), which was distilled over CaH_2 under nitrogen or HPLC grade acetonitrile (ACN) for the external reference. Absorption spectra were recorded at 298 K using a Shimadzu UV-1800 double beam spectrophotometer, or a HP-8453 diode array spectrophotometer or a Varian Cary 300 spectrophotometer. Molar absorptivity determination was verified by linear least squares fit of values obtained from at least three independent solutions at varying concentrations with absorbances ranging from 0.01-2.6. Steady-state emission and excitation spectra were recorded at 298 K and at 77 K in a 1.0 cm capped quartz cuvette and an NMR tube inserted into a liquid nitrogen filled quartz dewar, respectively. Emission spectra were obtained by exciting at the lowest energy absorption maxima using a Horiba Jobin Yvon Fluorolog-3 spectrofluorometer equipped with double monochromators and a photomultiplier tube detector (Hamamatsu model R955). Photon Technology International (PTI) and Fluorescence Quanta Master Series QM1 spectrophotometer have been also used to confirm the emission results. Emission quantum yields were determined using the optically dilute method.[6,7] A stock solution with absorbance of ca. 0.5 was prepared and then four dilutions were prepared with dilution factors of 40, 20, 13.3 and 10 to obtain solutions with absorbances of ca. 0.013, 0.025, 0.038 and 0.05, respectively. The Beer-Lambert law was found to be linear at the concentrations of the solutions. The emission spectra were then measured after the solutions were rigorously degassed with solvent-saturated nitrogen gas (N_2) for 20 minutes prior to spectrum acquisition using septa-sealed quartz cells from Starna. For each sample, linearity between absorption and emission intensity was verified through linear regression analysis and additional measurements were acquired until the Pearson regression factor (R^2) for the linear fit of the data set surpassed 0.9. Individual relative quantum yield values were calculated for each solution and the values reported represent the slope value. The equation $\Phi_s = \Phi_r(A_r/A_s)(I_s/I_r)(n_s/n_r)^2$ was used to calculate the relative quantum yield of each of the sample, where Φ_r is the absolute quantum yield of the reference, n is the refractive index of the solvent, A is the absorbance at the excitation wavelength, and I is the integrated area under the corrected emission curve. The subscripts s and r refer to the sample and reference, respectively. A solution of $[Ru(bpy)_3](PF_6)_2$ in ACN ($\Phi_r = 0.095$) was used as the external reference.[8] The experimental uncertainty in the emission quantum yields is conservatively estimated to be 10%, though we have found that statistically we can reproduce PLQYs to 3% relative error. The emission lifetimes were measured on a TimeMaster model TM-3/2003 apparatus from PTI. The source was a nitrogen laser with high-resolution dye laser (fwhm~1400 ps) and the excited lifetimes were obtained from deconvolution or distribution lifetimes analysis. Some samples were also measured using a

time-correlated single photon counting (TCSPC) option of the JobinYvon Fluorolog-3 spectrofluorometer, a pulsed NanoLED at 341 nm (pulse duration < 1 ns; fwhm = 14 nm), mounted directly on the sample chamber at 90° to the emission monochromator, was used to excite the samples and emitted light was collected using a FluoroHub from Horiba JobinYvon single-photon-counting detector. The luminescence lifetimes were obtained using the commercially available Horiba Jobin Yvon Decay Analysis Software version 6.4.1, software included within the spectrofluorimeter.

Computational Methodology. All density functional theory (DFT) calculations were performed with Gaussian 09[9]. The DFT geometry optimisations[10-19] were carried out using the B3LYP method. 6-31g* basis sets were used for the porphyrin, acetylene group, bipyridine and phenyl pyridine. 3-21g* basis sets were used for the solubilizing groups (phenyl groups of the porphyrin and PBu_3) that are attached to the Pt. VDZ (valence double ζ) with SBKJC effective core potentials were used for Zn, Pt and Ir.[20-25]

Electrochemical Characterization. Cyclic voltammetry analyses were performed on an Electrochemical Analyzer potentiostat model 600D from CH Instruments. Solutions for cyclic voltammetry were prepared in distilled ACN and degassed with ACN-saturated nitrogen bubbling for ca. 15 min prior to scanning. Tetra(n-butyl)ammonium hexafluorophosphate ($TBAPF_6$; ca. 0.1 M in ACN) was used as the supporting electrolyte. A non-aqueous Ag/Ag^+ electrode (silver wire in a solution of 0.1 M $AgNO_3$ in ACN) was used as the pseudo-reference electrode; a glassy-carbon electrode was used for the working electrode and a Pt electrode was used as the counter electrode. The redox potentials are reported relative to a saturated calomel (SCE) electrode with a ferrocenium/ferrocene (Fc^+/Fc) redox couple as an internal reference (0.40 V vs SCE).[26]

Table S1: Electrochemical data for **10** and **6.**

	E_{ox} /V		E_{red} /V			ΔE_{redox} /V
	E_{pa}^{1}/E_{pc}^{1}	E_{pa}^{2}/E_{pc}^{2}	E_{pa}^{1}/E_{pc}^{1}	E_{pa}^{2}/E_{pc}^{2}	E_{pc}^{3}/E_{pc}^{3}	
10	0.80/0.74	1.34/1.29	− /-0.91	-1.34/-1.40	-1.55/-1.61	1.71
6	0.76/0.70	1.32/1.26	− /-0.89	− /-1.36	-/-1.43	1.65

[a] Conditions: CVs recorded in N_2-saturated ACN at 298 K at a 200 mV/s scan rate with 0.1 M $(nBu_4N)PF_6$ as the supporting electrolyte. A non-aqueous Ag/Ag^+ electrode (silver wire in a solution of 0.1 M $AgNO_3$ in ACN) was used as the pseudoreference electrode; a glassy-carbon electrode was used for the working electrode, and a Pt electrode was used as the counter electrode. Waves are referenced vs Fc/Fc^+ as an internal standard and reported in V vs SCE (Fc/Fc^+ vs SCE = 0.40 V);[26] [b] Epa and Epc stand for anodic and cathodic peak potentials, respectively, with all waves found to be irreversible; [c] $\Delta E_{redox} = E_{pa}^{1,ox} - E_{pc}^{1,red}$.

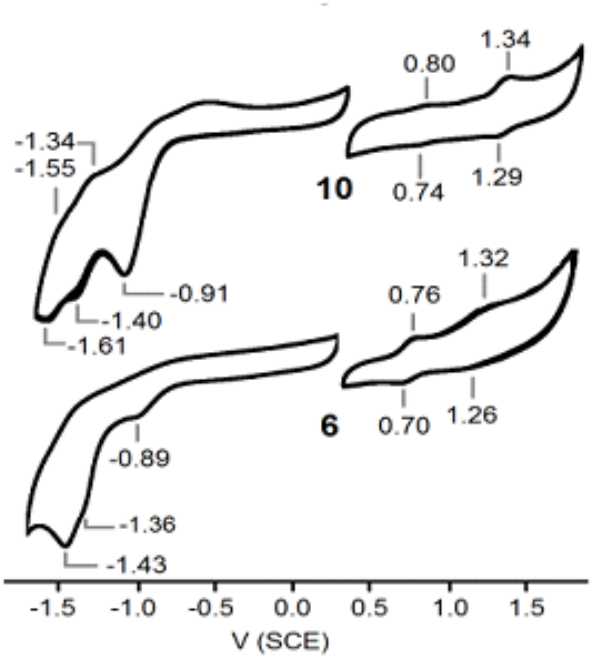

Figure S1: CV traces of **10** and **6** in degassed ACN at 298 K. Scan rate = 200 mV s^{-1}, with 0.1 M n-Bu_4NPF_6 as the supporting electrolyte.

Note on the Dexter mechanism. The Dexter energy transfer (introduced by David L Dexter) is sometimes called short-range energy transfer. It is a process that the donor and the acceptor exchange their electron. Hence, besides the overlap of emission spectra of donor and absorption spectra of acceptor, the exchange energy transfer needs the overlap of wavefunctions, meaning it needs the overlap of the electron cloud. The overlap of wavefunctions also implies that the excited donor and ground-state acceptor should be close enough so the exchange could occur. The rate constant of exchange energy transfer is given by $k_{Dexter} = KJ\exp(-2r_{DA}/L)$ where K is an experimental factor, r_{DA} is the center-to-center distance between the donor and acceptor, and L is the sum of van der Waals radius (r_{vdW}) of both chromophores and J is the spectral overlap integral calculated as:

$$J = \int f_{\mathrm{D}}(\lambda)\,\epsilon_{\mathrm{A}}(\lambda)\,\lambda^4\,d\lambda$$

where f_{D} is the normalized donor emission spectrum, and ϵ_{A} is the acceptor molar extinction coefficient.

For **1**, **5** and **6**, the structural parameters have been extracted from the optimized geometry of **3** (model complex) and **6** (DFT; B3LYP) below.

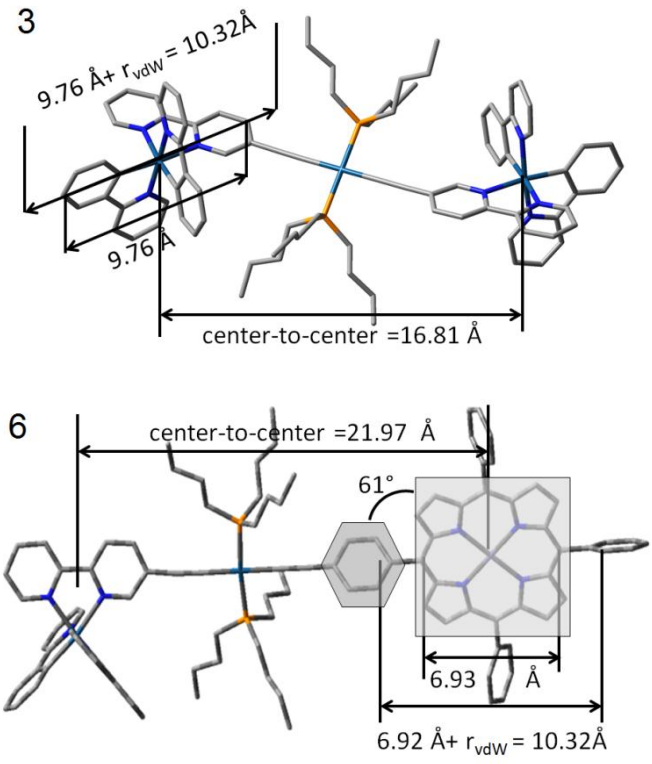

a

Figure S2: Optimized geometry of **3** and **6** (DFT; B3LYP) stressing on the r_{DA} and r_{vdW} data.

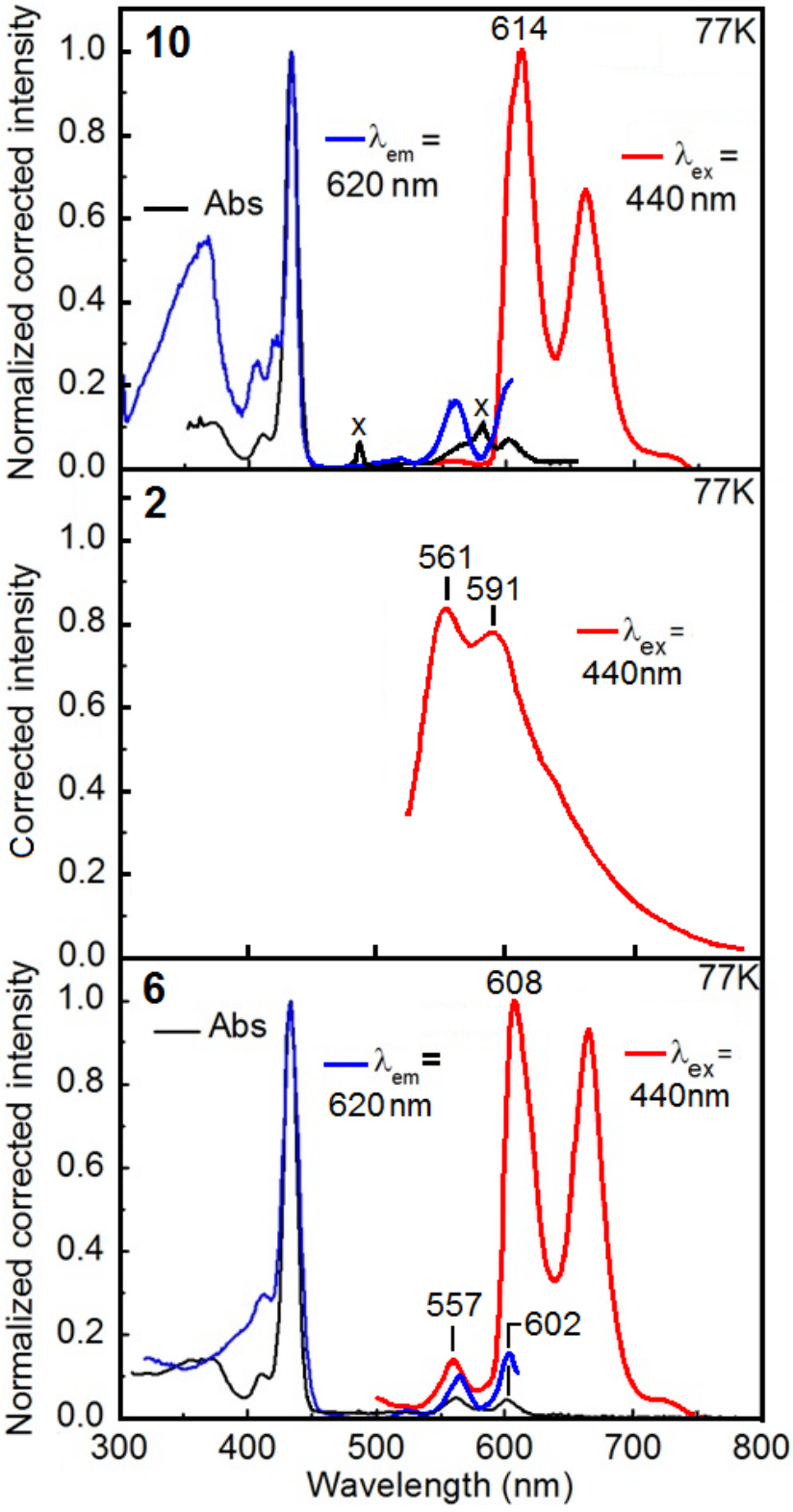

Figure S3: Absorption (black), emission (red) and excitation (blue) spectra of **10**, **2** (from ref. S27) and **6** in 2MeTHF at 77 K. The signals marked with an X are instrumental artifacts.

Compound 10

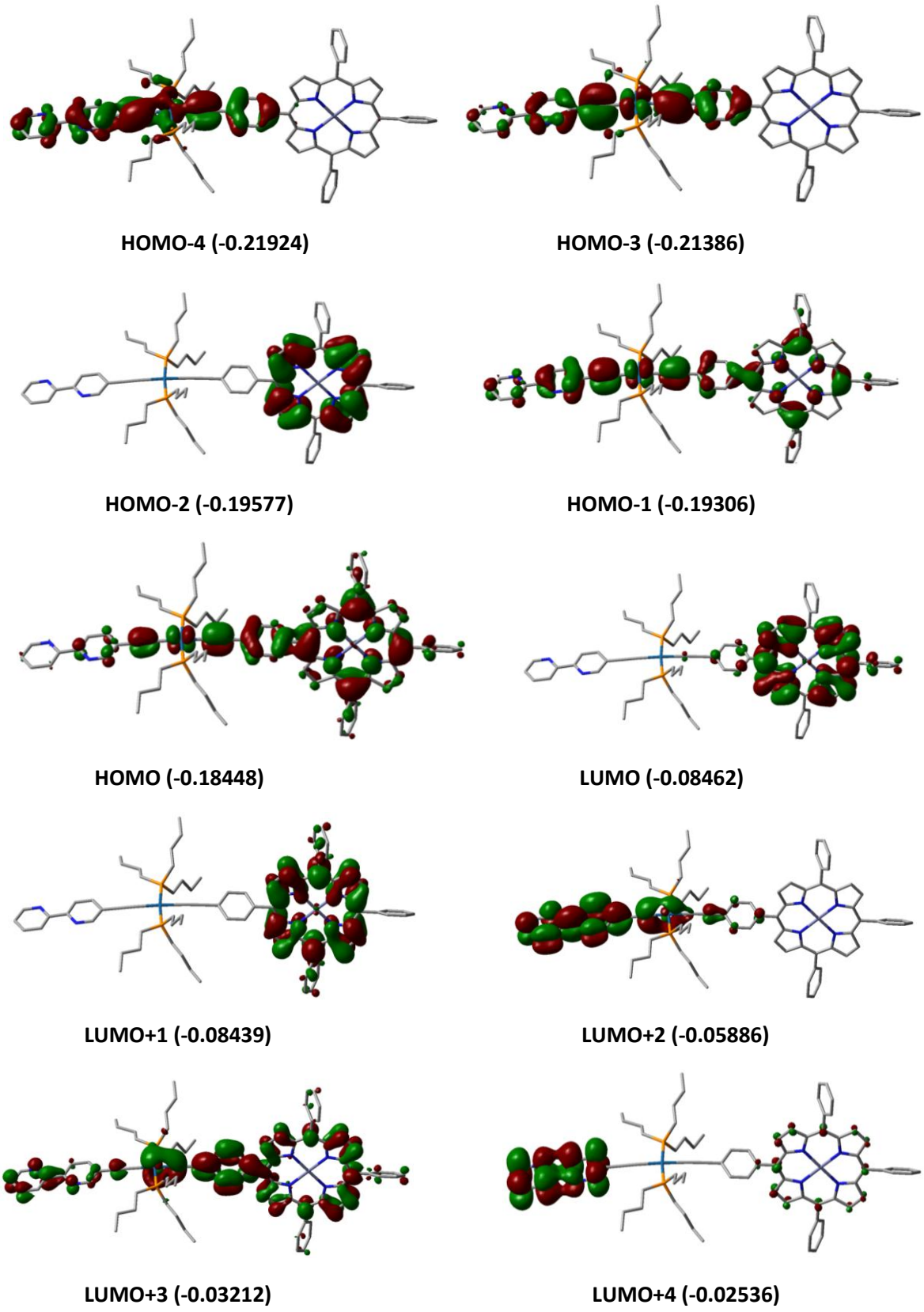

Figure S4. Representations of the frontier MOs for compound **10** (the energy is in a.u.)

Compound 6

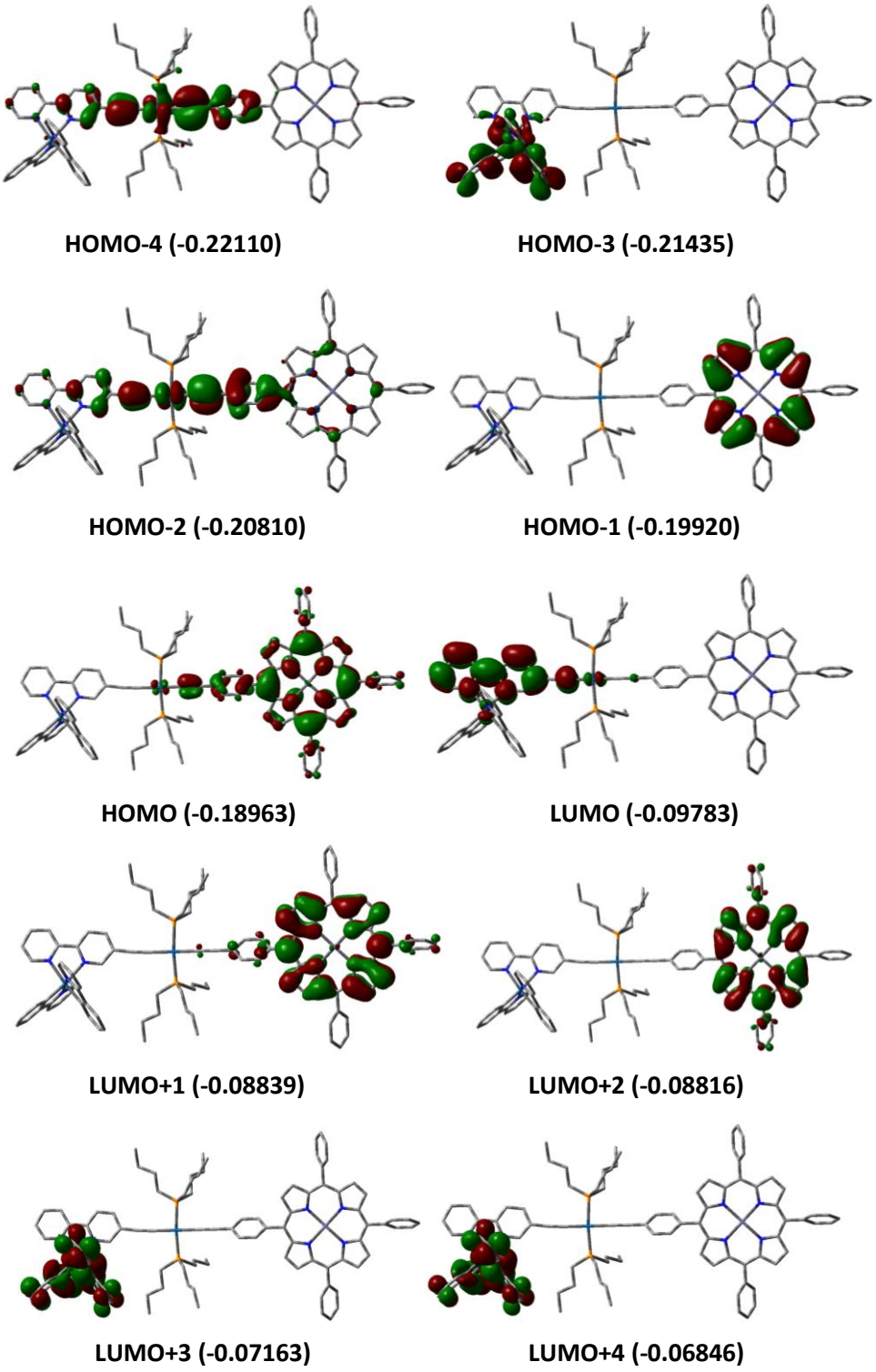

Figure S5. Representations of the frontier MOs for compound **6** (the energy is in a.u.)

Table S2: Atomic Contributions to the MOs:

The table below shows the % electronic contributions over given molecular fragments from HOMO-4 to LUMO+4. The fragments listed on the left of the table. The fragment exhibiting the largest atomic contributions is highlighted.

Compound 10

	H-4	H-3	H-2	H-1	HOMO	LUMO	L+1	L+2	L+3	L+4
Zinc- Porphyrin	16.0	15.1	97.2	36.0	66.1	91.2	87.4	3.6	62.4	7.7
Acetylene groups	38.7	46.6	0.01	24.5	11.6	0.4	0.0	7.8	6.6	0.4
Pt	10.3	18.6	0.00	17.6	7.4	0.1	0.00	5.0	5.7	0.6
Bipyridine	24.7	14.7	0.0	15.7	3.8	0.1	0.00	78.4	10.3	89.0
Solubilizing groups	10.3	5.0	2.8	6.3	11.1	8.2	12.58	5.3	15.1	2.3

Compound 6

	H-4	H-3	H-2	H-1	HOMO	LUMO	L+1	L+2	L+3	L+4
Zinc Porphyrin	17.4	0.0	30.1	97.2	81.0	0.6	91.0	87.5	0.0	0.0
Acetylene groups	43.8	0.5	35.7	0.0	2.8	5.1	0.4	0.0	0.0	0.1
Pt	23.1	0.2	21.3	0.0	0.9	2.0	0.1	0.0	0.0	0.0
Bipyridine	8.9	4.5	8.5	0.00	0.2	86.5	0.3	0.0	2.6	2.8
Phenylpyridine	0.3	49.5	0.1	0.0	0.0	2.5	0.0	0.0	92.9	92.3
Ir	0.4	45.2	0.2	0.0	0.0	2.1	0.0	0.0	4.2	4.6
Solubilizing groups	6.1	0.1	4.0	2.8	15.1	1.2	8.2	12.5	0.3	0.3

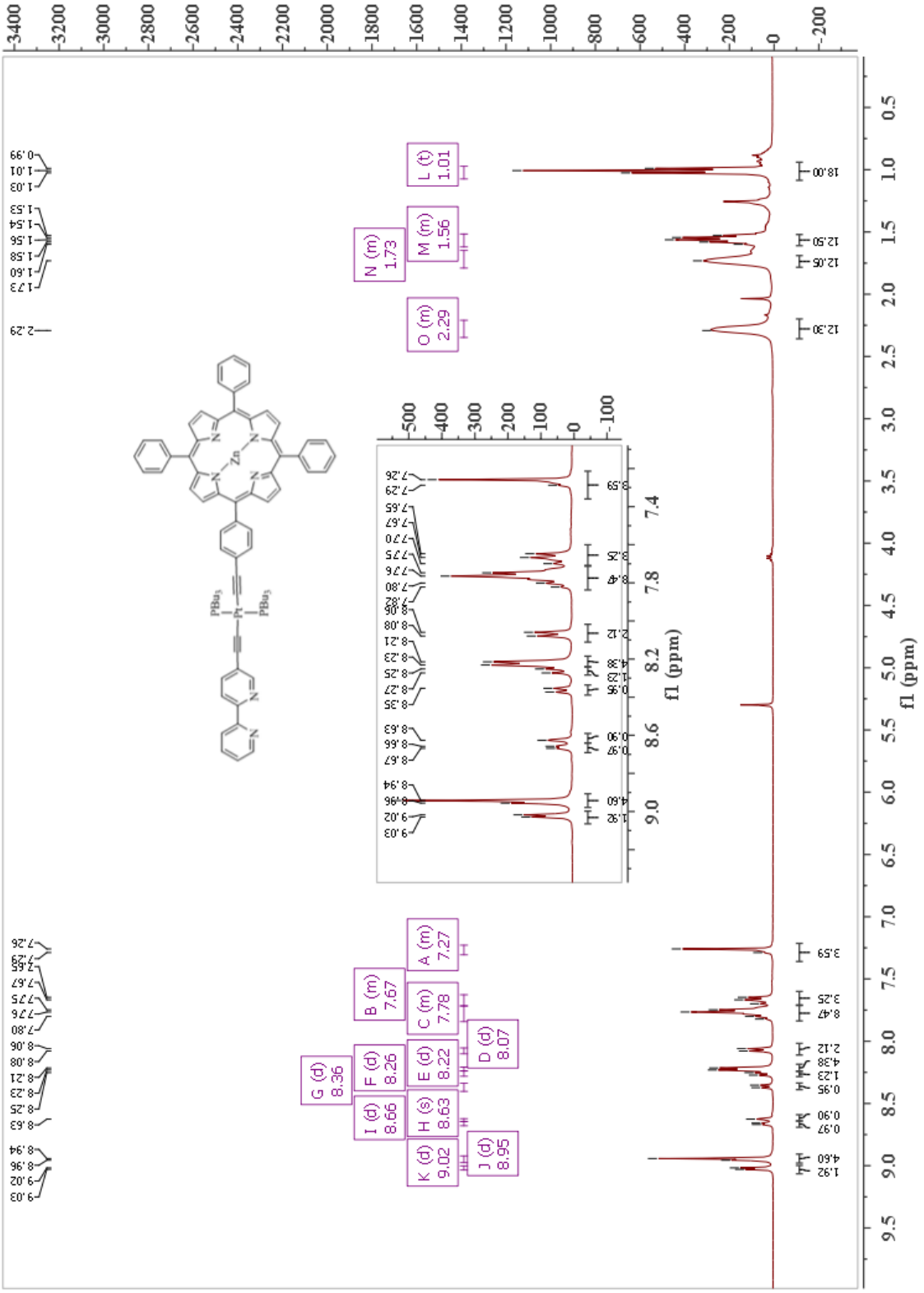

Figure S6: ^{1}H NMR data for**(10).**

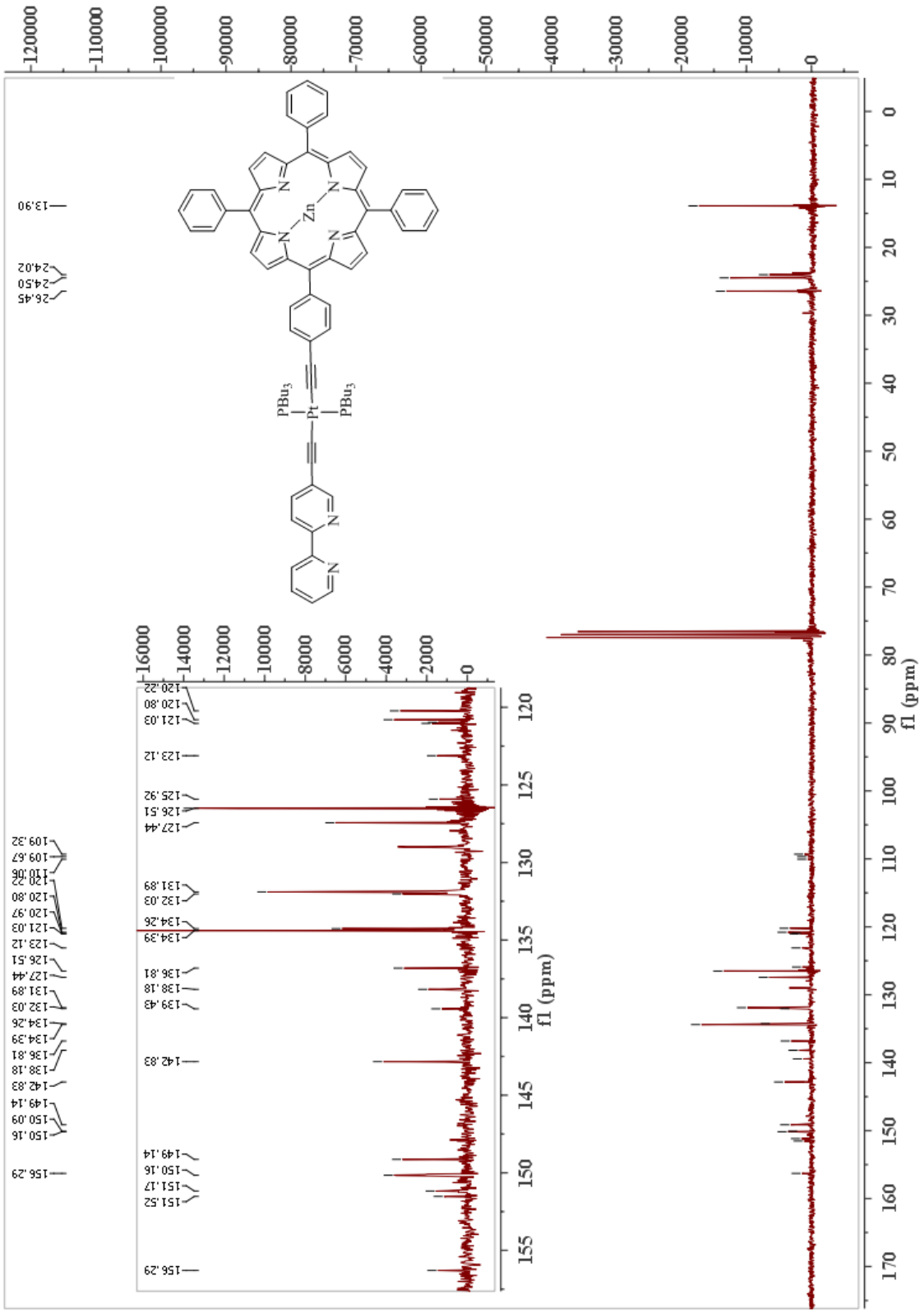

Figure S7: ^{13}C NMR data for **(10)**.

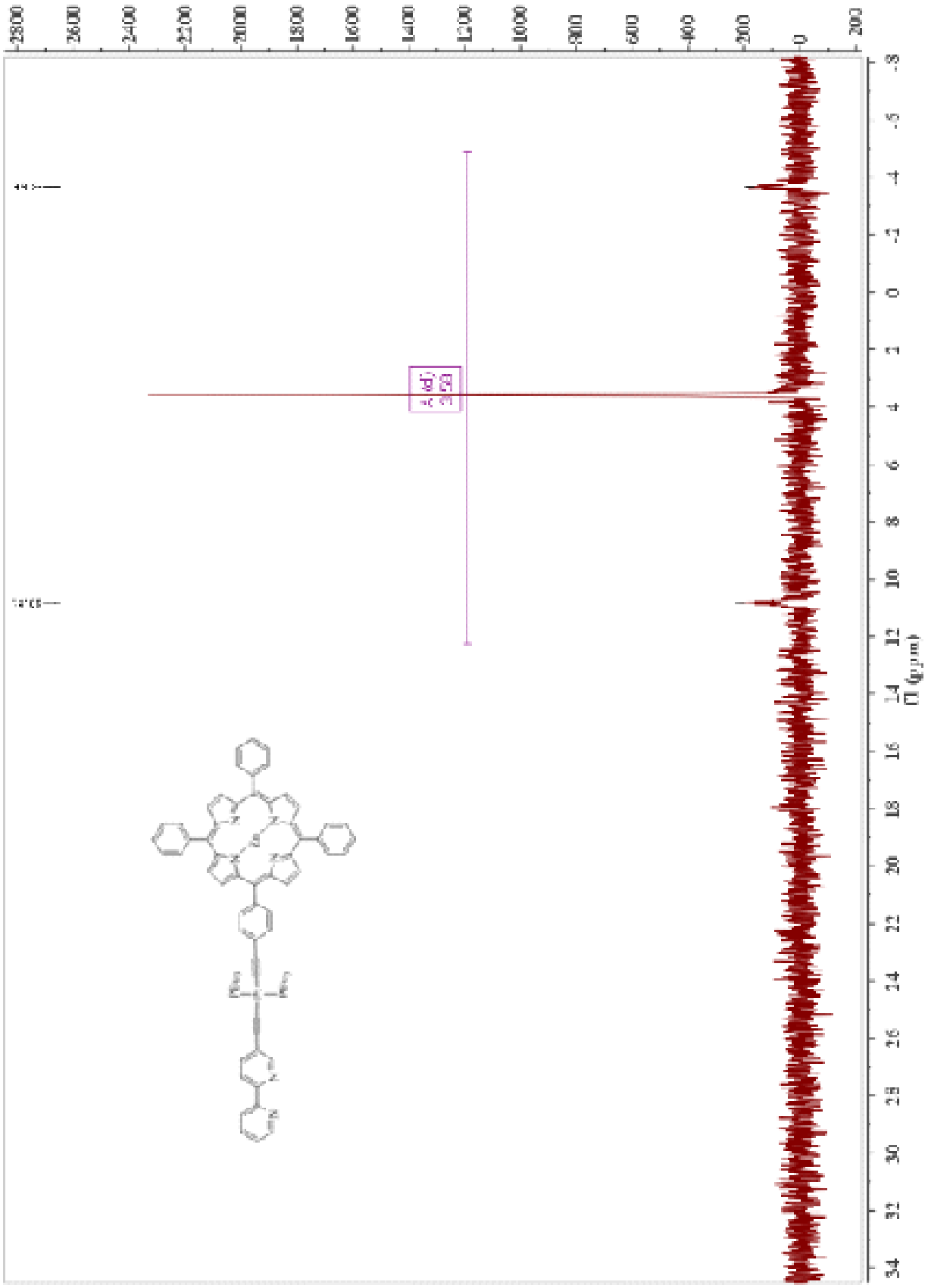

Figure S8: ^{31}P NMR data for**(10).**

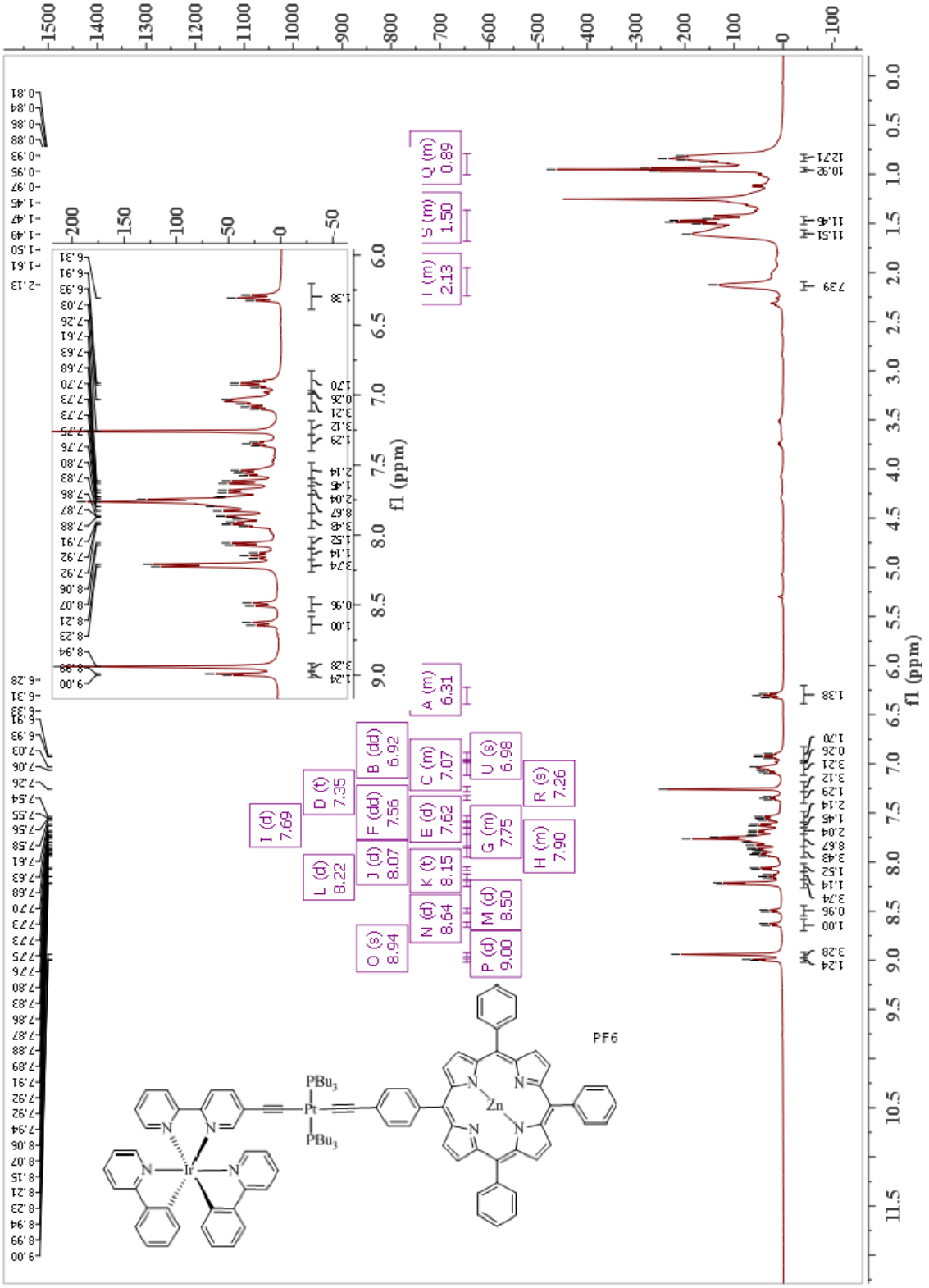

Figure S9: ^{1}H NMR data for**(6).**

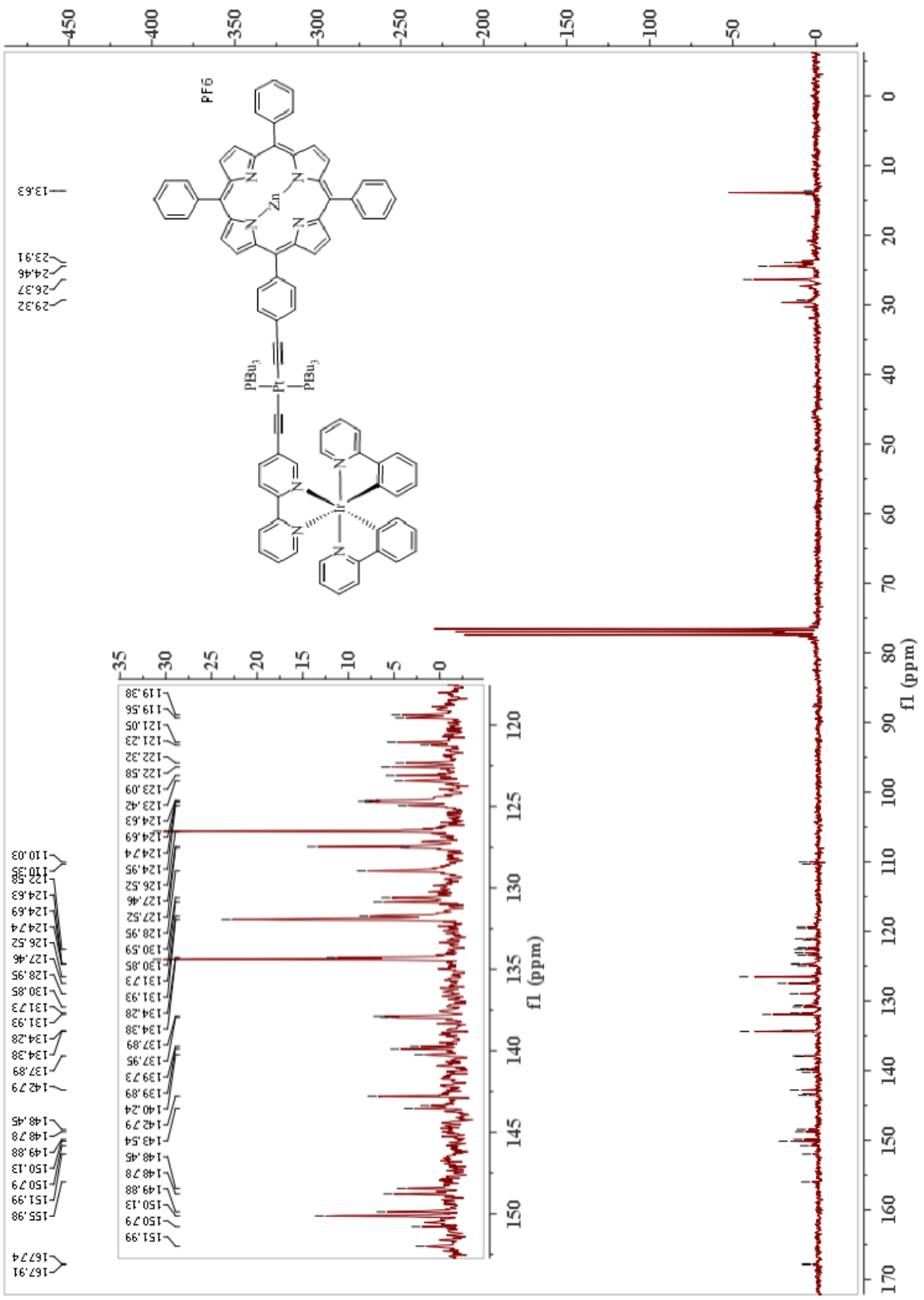

Figure S10: ^{13}C NMR data for**(6).**

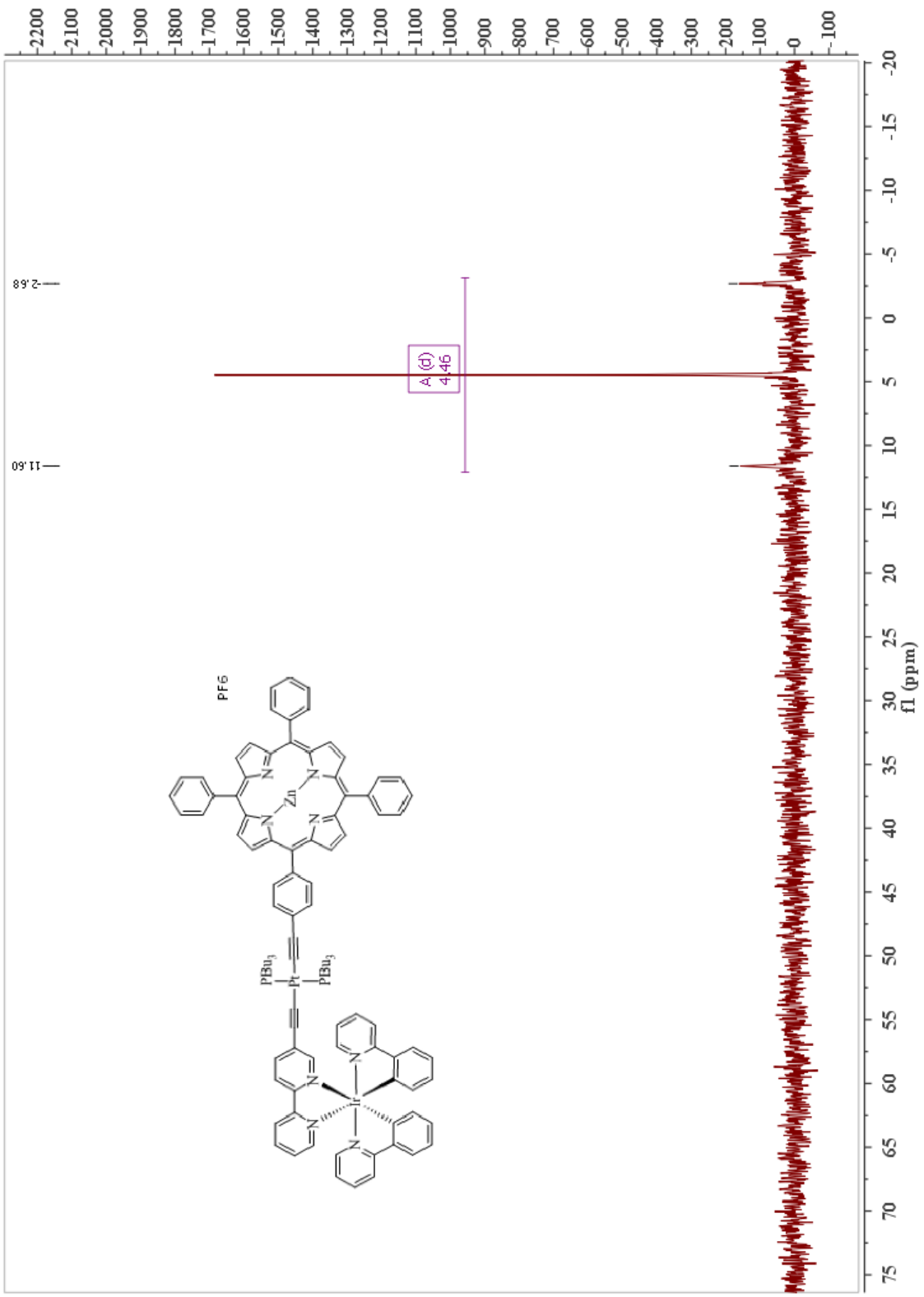

Figure S11: ^{31}P NMR data for**(6).**

References:

(1). G. B. Kauffman, L. A. Teter and J. E. Huheey, in *Inorg. Synth.*, John Wiley & Sons, Inc., 2007, pp. 245-249.
(2). W. L. F. Armarego and D. D. Perrin, *Purification of Laboratory Chemicals, 3rd edition*, Pergamon Press, Oxford, 1988.
(3). M. Nonoyama, *Bull. Chem. Soc. Japan*, 1974, **47**, 767.
(4). A. M. Soliman, D. Fortin, P. D. Harvey, and E. Zysman-Colman, *Chem. Commun.*, 2012, **48**, 1120.
(5). A. R. McDonald, N. Franssen, G. P. van Klink, G. van Koten, *J.Organomet. Chem.*, 2009, **694**, 2153.
(6). G. A. Crosby and J. N. Demas, *J. Phys. Chem.*, 1971, **75**, 991.
(7). S. Fery-Forgues and D. Lavabre, *J. Chem. Educ.*, 1999, **76**, 1260.
(8). H. Ishida, S. Tobita, Y. Hasegawa, R. Katoh and N. Nozaki, *Coord. Chem. Rev.*, 2010, **254**, 2449.
(9). M. J. Frisch *et al. Gaussian, Inc., Wallingford CT*, 2004.
(10). P. Hohenberg and W. Kohn, *Phys. Rev.* 1964, **136**, B864.
(11). P. Hohenberg and W. Kohn, *J. Phys. Rev.* 1965, **140**, A1133.
(12). R. G. Parr and W. Yang, *Density-functional theory of atoms and molecules*, Oxford Univ. Press: Oxford, 1989.
(13). D. R. Salahub and M. C. Zerner, *The Challenge of d and f Electrons, Amer. Chem. Soc. Washington, D.C.* 1989.
(14). R. Bauernschmitt and R. Ahlrichs, *Chem. Phys. Lett.* 1996, **256**, 454–464.
(15). M. E. Casida, C. Jamorski, K. C. Casida and D. R. Salahub, *J. Chem. Phys.* 1998, **108**, 4439.
(16). R. E. Stratmann, G. E. Scuseria and M. J. Frisch, *J. Chem. Phys.* 1998, **109**, 8218.
(17). C. Lee, W. Yang and R. G. Parr, *Phys. Rev. B.* 1988, **37**, 785.
(18). B. Miehlich, A. Savin, H. Stoll and H. Preuss,*Chem. Phys. Lett.* 1989, **157**, 200.
(19). A. D. Becke, *J. Chem. Phys.* 1993, **98**, 5648.
(20). J. S. Binkley, J. A. Pople and W. J. Hehre, *J. Am. Chem. Soc.* 1980, **102**, 939.
(21). M. S. Gordon, J. S. Binkley, J. A. Pople, W. J. Pietro and W. J. Hehre, *J. Am. Chem. Soc.* 1982, **104**, 2797.
(22). W. J. Pietro, M. M. Francl, W. J. Hehre, D. J. Defrees, J. A. Pople and J. S. Binkley, *J. Am. Chem. Soc.* 1982, **104**, 5039.
(23). K. D. Dobbs and W. J. Hehre, *J. Comput. Chem.* 1986, **7**, 359.
(24). K. D. Dobbs and W. J. Hehre, *J. Comput. Chem.* 1987, **8**:, 861.
(25). K. D. Dobbs and W. J. Hehre, *J. Comput. Chem.* 1987, **8**:, 880.
(26). N. G. Connelly and W. E. Geiger, *Chem. Rev.* 1996, **96**, 877.
(27) A. M. Soliman, D. Fortin, P. D. Harvey, and E. Zysman-Colman *Chem.Comm.*, 2012, **48**, 1120.